Modeling the Excitation of Fibers Under Surface Electrodes

FRANK RATTAY

Abstract—**In my previous work, it was shown that the electrostimulation of nerve or muscle fibers is caused by the activating function which is the second differential quotient of the extracellular potential along the fiber. To find the activating function, a simple model is used to approximate in an homogeneous medium the potential distribution produced by a surface electrode. Data from classical space-clamped experiments allow calculation of fiber response as a function of geometry and stimulating signal shape.**

Introduction

THE tools for functional electrostimulation are implanted electrodes or transcutaneous ones. By such electrodes, a space and time-depending potential V_e is caused in the medium where the nerve and muscle fibers are imbedded. In previous papers, it was shown that the reaction of any unmyelinated fiber is determined by the second derivative of the extracellular potential along the fiber (d^2V_e/dx^2) whereas the activation for myelinated fibers results from the second difference quotient $\Delta^2V_e/\Delta x^2$ [1], [2].

We find this important result from an electrical network for the current flow across the membrane of the fiber (Fig. 1). The current flow for the nth segment of the fiber at the point marked with a full circle is caused by the voltages between the different points of the network, and consists of a capacitance current, an ionic current, and a current along the inside. (Symbols and units are listed in Table I.)

$$C_m \cdot d(V_{i,n} - V_{e,n})/dt + I_{i,n} + G_a(V_{i,n} - V_{i,n-1}) + G_a(V_{i,n} - V_{i,n+1}) = 0. \quad (1)$$

We introduce the reduced voltages

$$V_n = V_{i,n} - V_{e,n} + V_{\text{rest}} \quad (2)$$

and find

$$dV_n/dt = \{G_a(V_{n-1} - 2V_n + V_{n+1} + V_{e,n-1} - 2V_{e,n} + V_{e,n+1}) - I_{i,n}\}/C_m. \quad (3)$$

By inserting $G_a = \pi d^2/4\rho_i\Delta x$ and $C_m = \pi dLc_m$ and introducing the ionic current density $i_{i,n}$, (3) reads as

Manuscript received April 3, 1987, revised September 9, 1987.

The author is with the Institut für Analysis, Technische Mathematik und Versicherungmathematik, Technical University of Vienna, A-1040 Vienna, Austria.

IEEE Log Number 8718587.

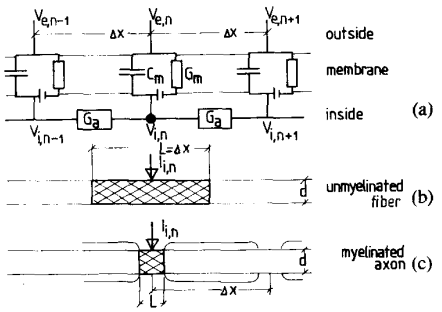

Fig. 1. Electrical network to simulate the currents in an axon. Unmyelinated as well as myelinated fibers are segmented into cylinders of length Δx. Whereas Δx is given by the internodal distance in the myelinated case, Δx depends only on computational accuracy for unmyelinated fibers. Within one segment the membrane is active in the cross-hatched area. The membrane of every cylinder is simulated by an electric circuit (top diagram) consisting of capacity C_m, ionic voltage source, and the nonlinear conductance G_m. G_a symbolize the conductance of axoplasm between two segments. $V_{e,n}$ and $V_{i,n}$ are the external and the internal potential of the nth segment.

$$\frac{dV_n}{dt} = \left\{\frac{d}{4\rho_i} \cdot \left(\frac{V_{n-1} - 2V_n + V_{n+1}}{\Delta x \cdot L} + \frac{V_{e,n-1} - 2V_{e,n} + V_{e,n+1}}{\Delta x \cdot L}\right) - i_{i,n}\right\}\Big/c_m. \quad (4)$$

The ionic currents i_i will be described by further differential equations, e.g., the Hodgkin–Huxley equations for the unmyelinated case or the Frankenhaeuser–Huxley equations for the myelinated fiber [3]–[5].

Equation (4) shows that the influence from extracellular current sources is given by

$$f_n(t) = \frac{V_{e,n-1} - 2V_{e,n} + V_{e,n+1}}{\Delta x \cdot L} \quad (5)$$

where L is the nonisolated length of membrane in one segment [Fig. 1(b) and (c)]. L is the nodal gap width and Δx is the internodal length for myelinated fibers. In the case of unmyelinated fibers, $L = \Delta x$, and with $\Delta x \to 0$, (5) reads as

$$f(x, t) = \partial^2 V_e(x, t)/\partial x^2. \quad (6)$$

We will call $f(x, t)$ the activating function because it is responsible for activating a fiber by extracellular stimulation. To get an action potential by extracellular stimu-

TABLE I
SYMBOLS AND [UNITS]

C_m	capacity of membrane	[μF]
c_m	capacity of membrane per cm^2	[μF/cm^2]
G_a	conductance of axoplasm	[kΩ]
ρ_i	resistivity of axoplasm	[k$\Omega \cdot$ cm]
$V_{i,n}$	internal potential	[mV]
$V_{e,n}$, V	external potential	[mV]
V_n	reduced voltage (2)	[mV]
$I_{i,n}$	total ionic current	[μA]
x	length coordinate of the fiber	[cm]
Δx	segment length of the fiber	[cm]
L	active length of membrane	[cm]
d	fiber diameter	[cm]
i_i	total ionic current density	[μA/cm^2]
z	distance to the surface (depth)	[cm]
r	distance from the axis of the electrode	[cm]
a	radius of electrode	[cm]
V_0	potential under the electrode (Fig. 2)	[mV]
f_n	extracellular stimulus at nth segment (5)	[mV/cm^2]
f	activating function (6)	[mV/cm^2]
t	time	[ms]

lation in a fiber which is at rest, V_n [(2)] has to become positive. Therefore, according to (4), an action potential can be generated at the fiber coordinate $x_n = n \cdot \Delta x$ when f_n is positive. In areas where f_n is negative, hyperpolarization is produced. Because $f_n(t)$ of (5) may be approximated by $f(n \cdot \Delta x, t)$ [which is the activating function of (6)] the response of myelinated and unmyelinated fibers to extracellular stimulation is quite similar qualitatively as long as f does not vary too much within the nodal distance Δx [2]. (Δx is in the order of 1 mm.) Strong variations of f occur especially in the case of small implanted electrodes positioned close to the fiber. Here the reactions of myelinated fibers depend on the distance to a node of Ranvier. A discussion of current–distance phenomena resulting from implanted spherical electrodes is done in [2]. An examination of cuff-electodes is also possible with the help of the activating function and the results will be presented in a forthcoming paper.

The present paper is concerned with modeling the stimulation of fibers by transcutaneous disk electrodes. We will assume an homogeneous isotropic extracellular medium where the extracellular potential is determined by electrode current.

An Idealized Model for Surface Electrodes

To analyze reactions of the fibers in the vicinity of surface electrodes, we simplify the geometry. In order to avoid complications with the nonuniform resistance of the skin, we neglect the current spread within the thin sheets of the skin and assume constant potential V_0 in that surface domain of the conducting medium under the skin which lies just below the electrodes (Fig. 2). The semi-infinite homogeneous medium where the nerve and muscle fibers are imbedded may contain a grounded electrode at infinity. We will examine the quasi-static case (where the biological tissue impedances are purely resistive) in order to find the extracellular potential with respect to that special fiber which will be studied.

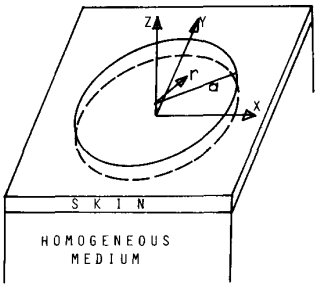

Fig. 2. Geometry of the electrode to be analyzed. A circular electrode of radius a is symbolized by the full curve. The semi-infinite homogeneous conductive medium under the electrode is separated by the skin. We neglect the current spread within the skin and assume constant voltage V_0 within the circle (broken line) at that part of the surface of the homogeneous medium which lies under the electrode.

To find the potential V we solve Laplace's equation

$$\Delta V = 0. \tag{7}$$

For electrical potentials with axial symmetry, the solution is of the form

$$V(r, z) = \int_0^\infty A(k) \cdot e^{-k|z|} J_0(kr)\, dk \tag{8}$$

with the Bessel function J_0 and suitable $A(k)$ to satisfy the boundary conditions. In our case they are

$$V = V_0 \quad \text{for } z = 0,\ r \le a \tag{9a}$$

$$\partial V/\partial z = 0 \quad \text{for } z = 0,\ r > a \tag{9b}$$

and

$$V \to 0 \quad \text{for } r \to \infty,\ z \to -\infty. \tag{9c}$$

Equation (8) has the following analytic solution [6]

$$V(r, 0) = V_0 \quad \text{for } r \le a \tag{10a}$$

in the surface domain under the electrode and

$$V(r, z) = \frac{2V_0}{\pi} \cdot \arcsin\left\{\frac{2a}{\sqrt{(r-a)^2 + z^2} + \sqrt{(r+a)^2 + z^2}}\right\} \tag{10b}$$

everywhere else. Having in mind that the solution is symmetrical to rotation, we will simplify the geometry by selecting a special direction which defines the x axis (Fig. 2).

Fig. 3(a) shows the potential V at x lines in planes parallel to the surface at the depths $z = -a/10$ and $z = -a/2$. The corresponding activating functions for excitable fibers which are positioned at those x lines are plotted in Fig. 3(b). As the voltage drops fast at the edge of the electrode, the shape of the electrode is seen especially in the upper traces of Fig. 3(a) and (b). At a constant depth, the strongest reactions are at the lines which intersect the

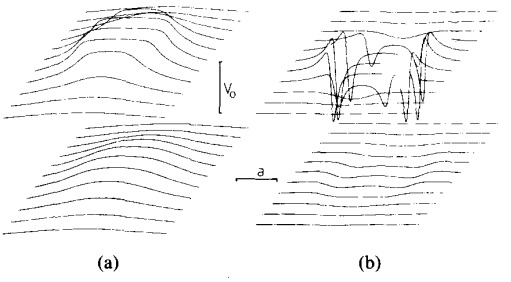

Fig. 3. (a) Potential distribution at x lines as part of V_0 at the depth $z = -a/10$ (upper diagram) and at $z = -a/2$. (b) Activating functions at the x lines as in (a).

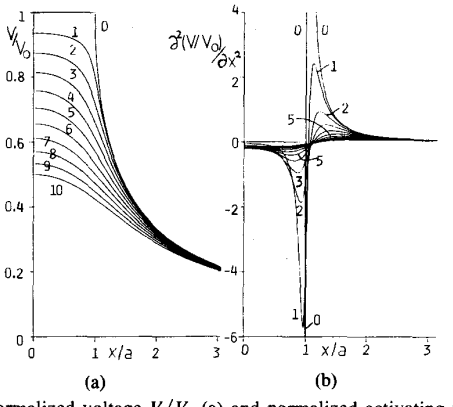

Fig. 4. Normalized voltage V/V_0 (a) and normalized activating function $\partial^2(V/V_0)/\partial x^2$ in the x-z plane as functions x/a. For $z/a = 0, 0.1, 0.2, \cdots 1$, the curves are marked with numbers 0, 1, 2, $\cdots$, respectively. At $z = 0$ the voltage is constant under the electrode but decreases with a vertical decay at $x = a$ and the activating function becomes infinite there. All the curves are symmetrical with respect to $x = 0$.

z axis ($y = 0$). Fig. 4(a) and (b) shows V and the activating functions $\partial^2 V/\partial x^2$ (scaled by V_0) for $y = 0$ and $z/a = 0, 0.1, 0.2, \cdots 1$. As the activating function shrinks with depth, higher voltages at the electrode are necessary to stimulate the deep fibers. The threshold voltages are listed in Table II for cathodal (V_0^-) and anodal (V_0^+) stimulation. For fibers lying parallel to the surface in the depth z under the center of the electrode, the voltage–distance relation is fairly linear. As mentioned above, spikes will be generated in areas where the activating function is positive. If $V_0 > 0$, their (two symmetrical) places of origin will be within the intervals $a < |x| < 2a$ where $\partial^2(V/V_0)/\partial x^2 > 0$ [Fig. 4(b), 5(b)], but for $V_0 < 0$ the activating function changes the sign and spikes are generated at $|x| < a$ where $-\partial^2(V/V_0)/\partial x^2 < 0$ [Figs. 4(b) and 5(a)]. Fig. 4(b) shows that the activating functions have stronger excursions into the negative domain and, therefore, thresholds are smaller for cathodal stimulation than for anodal.

Discussion

We have mentioned above that modeling of fibers with and without myelin sheets is very similar. The difference consists in the use of difference, respectively, differential quotients of second order to describe the influence of the extracellular potential. Surface electrodes used for functional electrostimulation have a size on the order of centimeters and, therefore, the width of the depolarizing (positive) part and the hyperpolarizing (negative) part of the activating function are also on the order of centimeters [Figs. 3(b) and 4(b)]. Replacing the second difference quotient f_n [(5)] by the corresponding differential quotient, or even shifting the nodes in x direction, e.g., by the length $\Delta x/2$, will not change the firing responses essentially. This means that the results do not depend on the segmentation as long as Δx is on the order of 1 mm or smaller.

The effects resulting from the nonlinear conductances of the ionic currents are more striking. Comparing the

TABLE II
Threshold Voltages as a Function of z

z [cm]	(a) V_0^- [V]	(a) V_0^+ [V]	(a) $-V_0^+/V_0^-$	(b) V_0^- [V]	(b) V_0^+ [V]	(b) $-V_0^+/V_0^-$
0.1	−0.9	1.8	2	−0.45	0.7	1.5
0.2	−1.8	3.4	1.9	−0.7	0.9	1.3
0.3	−2.7	4.4	1.6	−0.9	1.3	1.4
0.4	−3.8	6.2	1.6	−1.1	1.7	1.5
0.5	−5.2	8.5	1.6	−1.5	2.2	1.5
1	−11.2	29	2.5	−2.8	6	2.1

(a) The values were calculated with Frankenhaeuser standard data but $T = 37°C$, $d = 5\ \mu m$, $\rho_i = 100\ \Omega \cdot cm$, $\Delta x = 1$ mm, $L = 2.5\ \mu m$, and $a = 1$ cm.

(b) Calculation with standard Hodgkin-Huxley data but $T = 29°C$, $\Delta x = 1$ mm and $a = 1$ cm.

Stimulation was simulated with single square pulses of 100 μs in all the cases.

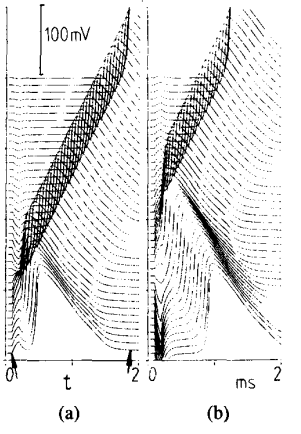

Fig. 5. Fiber reaction to negative square pulse ($V_0 = -6$ V) (a) and to a positive pulse ($V_0 = 12$ V) (b) calculated according to the network of Fig. 1 and to (10). (Standard Frankenhaeuser data, but $d = 5\ \mu m$, $T = 37°C$, duration of impulse: 100 μs, $a = 1$ cm, $z = -0.5$ cm, nodal separation $\Delta x = 1$ mm, $L = 2.5\ \mu m$, $\rho_i = 100\ \Omega \cdot cm$.) Every line corresponds to the reaction at a node. The lowest line shows the reduced voltage V across the membrane [(2)] at $x = 0$, the next one at $x = 1$ mm etc. until $x = 40$ mm. For negative x values, the result is a mirror image of the one shown. Within the stimulation time from $t = 0.1$ ms to $t = 0.2$ ms, the conductance of the membrane is nearly constant because the stimulus signal is just a little above threshold and we can recognize the image of the corresponding activating function marked by number 5 in Fig. 4(b). Arrows mark the voltage before ($V = 0$) and after an action potential ($V > 0$, no hyperpolarization).

columns of Table II, we see that the ratio of anodal to cathodal threshold voltage in the Hodgkin–Huxley model [case (b)] is smaller than that for the Frankenhaeuser–Huxley model. The lowest trace of Fig. 5(a) shows the reaction of a fiber stimulated with a negative pulse. The fiber is at rest before it is stimulated, but after a stimulus pulse of 100 μs, V will be always positive [arrows in Fig. 5(a)]. This means that in the Frankenhaeuser–Huxley model the "natural" shape of a spike has no hyperpolarized region, which is in contrast to the Hodgkin–Huxley axon (arrows in Fig. 6). More generally, we can say that the Hodgkin–Huxley membrane is more sensitive to hyperpolarization than the Frankenhaeuser–Huxley membrane. To explain the "hyperpolarizing effect," we will compare the first line of Table II with the corresponding activating function marked by 1 for $z/a = 0.1$ of Fig. 4(b). The negative part of the scaled activating function $\partial^2(V/V_0)/\partial x^2$ is more than twice as strong than the positive one [Fig. 4(b)], and the ratio of the threshold voltages is $V_0^+/V_0^- = 2$. The threshold voltage V_0^+ to excite the giant Hodgkin–Huxley axon at the same position ($z = -1$ mm) is 0.7 V, but a -0.35 V pulse is too weak to overcome the hyperpolarized region. By line 1 of Table II, we find the ratio $V_0^+/V_0^- = 1.5$.

In [2], the author had shown that unmyelinated fibers will not produce a propagating spike when stimulated with a negative current greater than eight times threshold coming from an implanted spherical electrode. This happens because the "action potential" is sent into a hyperpolarized region of the axon which stops the activity. This effect is known experimentally for the unmyelinated [7] as well as for the myelinated fiber [8], [9]. We can get this blocking phenomenon by computation with the Hodgkin–Huxley membrane but not with the equations for the ionic currents proposed by Frankenhaeuser and Huxley. Therefore, we must conclude that the Frankenhaeuser–Huxley model fails for suprathreshold stimulation as far as sensitivity to hyperpolarization is concerned.

Fig. 5 shows the response of a fiber for $x > 0$ when stimulated with negative V_0 (a) and positive V_0 pulse (b) just above threshold. The place of the origin of the spike is at the maximum of the activating function which corresponds to the minimum of curve 5 of Fig. 4(b) for negative stimulus [Fig. 5(a)], and to the maximum of curve 5 of Fig. 4(b) for positive stimulus [Fig. 5(b)]. By the different places of generation, different time delays are caused at the point of destination. Applying strong cathodal stimuli will not change the firing behavior predicted by the Frankenhaeuser–Huxley model. In contrast, in the Hodgkin–Huxley model propagation will be stopped by the hyperpolarized area for this case (Fig. 6).

Under the assumptions made in this paper, we can conclude that if the positive threshold voltages are on the same order as the negative ones, the membrane is sensitive to hyperpolarization and we will get the blocking phenomenon for strong cathodal stimuli in fibers close to the surface.

The type of electrode discussed is not well suited for stronger stimuli because high current densities leading to burning problems occur at the edge [6], [10]. Better results will be obtained by electrodes where V_0 is not constant over the whole area but where V_0 is a function of r and V_0 drops towards the edge. In these cases, the potential lines of Fig. 4(a) will lose their small radii of curvature for small values of z, and the activating function which is related to the reciprocal value of these radii will become smaller there.

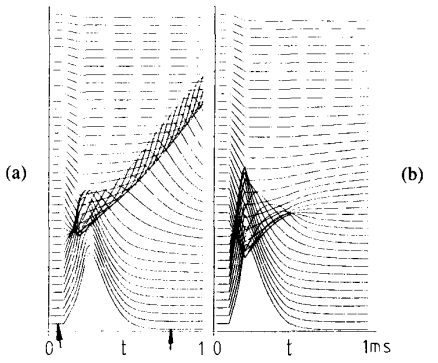

Fig. 6. Reaction of the fiber simulated by the Hodgkin–Huxley model and calculated as in Fig. 5, based on the data of Table II, for $z = -0.5$ cm with a stimulus voltage of -5 V (a) and -10 V (b) (Threshold: $V_0 = -1.5$ V). Fiber activity will not propagate in (b) because the spike cannot travel across the strongly hyperpolarized region (See text). Arrows mark the voltage before ($V = 0$) and after an action potential ($V < 0$, hyperpolarization).

References

[1] F. Rattay, "Analysis of models for external stimulation of axons," *IEEE Trans. Biomed. Eng.*, vol. BME-33, pp. 974–977, 1986.
[2] ——, "Ways to approximate current-distance relations for electrically stimulated fibers," *J. Theor. Biol.*, vol. 125, pp. 339–349, 1987.
[3] A. L. Hodgkin and A. F. Huxley, "A quantitative description of membrane current and its application to conduction and excitation in nerve," *J. Physiol. (London)*, vol. 117, pp. 500–544, 1952.
[4] B. Frankenhaeuser and A. F. Huxley, "The action potential in the myelinated nerve fiber of Xenopus Laevis as computed on the basis of voltage clamp data," *J. Physiol. (London)*, vol. 171, pp. 302–315, 1964.
[5] J. J. Jack, D. Noble, and R. W. Tsien, *Electric Current Flow in Excitable Cells*. Oxford, England: Clarendon, 1975.
[6] J. D. Wiley and J. G. Webster, "Analysis and control of the current distribution under circular dispersive electrodes," *IEEE Trans. Biomed. Eng.*, vol. BME-29, pp. 381–385, 1982.
[7] B. Katz and R. Miledi, "Propagation of electrical activity in motor nerve terminals," in *Proc. Roy. Soc. B*, vol. 161, pp. 453–482, 1965.
[8] W. J. Roberts and D. O. Smith, "Analysis of threshold currents during microstimulation of fibres in the spinal cord," *Acta Physiol. Scand.*, vol. 89, pp. 384–394, 1973.
[9] J. B. Ranck, Jr., "Which elements are excited in electrical stimulation of mammalian central nervous system: A review," *Brain Res.*, vol. 98, pp. 417–440, 1975.
[10] K. M. Overmyer, J. A. Pearce, and D. P. DeWitt, "Measurement of temperature distributions at electro-surgical dispersive electrode sites," *Trans. ASME, J. Biomech. Eng.*, vol. 101, pp. 66–72, 1979.

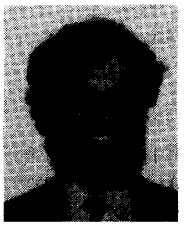

Frank Rattay was born in Tyrol, Austria, on May 29, 1945. He studied geodesy and technical mathematics and received the Dipl. Ing., Dr. techn., and Habilitation degrees from the Technical University of Vienna, Vienna, Austria, in 1974, 1980, and 1987, respectively.

Since 1972 he has been with the Institute of Analysis, Technische Mathematik und Versicherungsmathematik of the Technical University of Vienna. His main scientific interests include electrostimulation, hearing theory and speech features. Additionally, he has served as a consulting engineer for projects in underdeveloped countries.